

Development of a High Throughput 3D *in vitro* Wound Healing Model

Application Note

The skin is human's body largest organ and fulfills many functions, with its main purpose to provide a protective barrier against the external environment. After injury, the skin has a self-regenerative mechanism, the wound healing process, consisting of 4 phases. Immediately after injury, the hemostasis phase begins. Blood fills the wound and aggregated platelets and red blood cells form a thrombus, which stops the bleeding and facilitates

a provisional matrix for the next steps in the wound healing process. Next, in the inflammatory phase (Fig. 1), the wound environment is cleaned from damaged cells and tissue, including glycosaminoglycans (GAG). The proliferative phase includes the migration of cells into the wound as well as the production of new extracellular matrix (ECM), resulting in wound closure. This increases the number of cells in the wound environment as well as ECM

products, such as collagen and GAGs (Fig. 1). Lastly, the fibroblast-produced tissue matures in the maturation phase. The interaction between various cell types is of high importance to facilitate proper and complete wound closing and healing (Fig. 1). Especially the interplay between fibroblasts, or connective tissue cells, and keratinocytes (epidermal skin cells) is crucial [1].

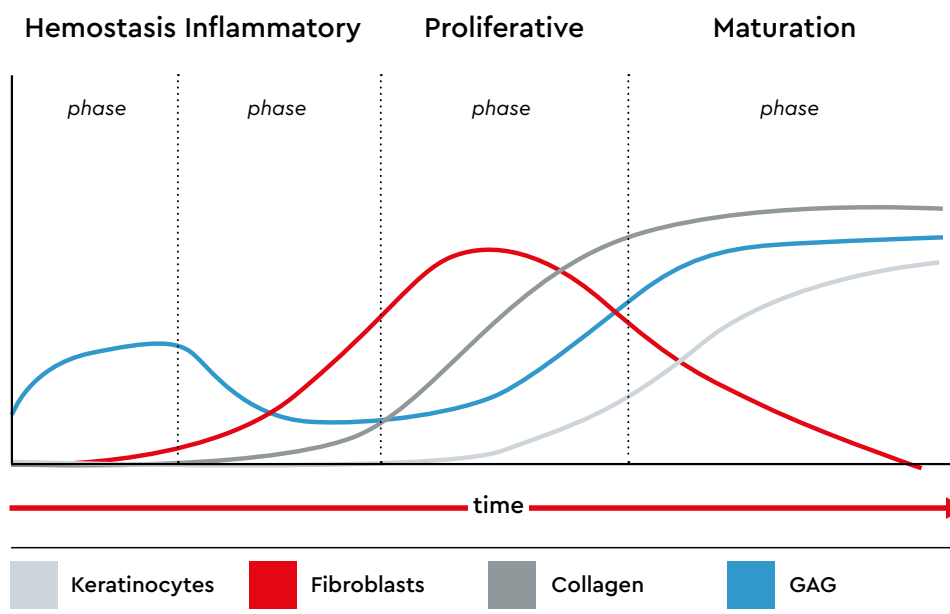


Fig. 1: An overview of the presence of keratinocytes, fibroblasts, GAGs and collagen in all phases of the native wound healing process. The amounts are based on a literature study [1].

Current therapies for chronic or severe wounds are generally painful, high in cost and enclose a long and often incomplete recovery. Abundant research is performed to overcome these limitations, however, *in vitro* models still have several limitations [2,3]. One of the main limitations in *in vitro* research is the use of 2D wound healing models, which lack the ability to mimic the physiological and structural native cellular environment [4]. Therefore, a switch to 3D *in vitro* research is necessary. However, present 3D wound healing models are often highly laborious and require high technical skills [5]. In addition, existing *in vitro*

wound healing models do not take the different phases into account while drugs can have a different impact on each phase [6]. Overall, a relatively easy 3D wound healing model to investigate the different phases and cell types of the wound healing process, is required. The Magnetic 3D Bioprinting technique from Greiner Bio-One can be used to easily create 3D cellular constructs. In addition, using different ratios of cell types helps to mimic the different phases of wound healing into one model. To understand and capture the complete 3D wound healing process, automated live cell imaging in combination with

a high temporal resolution is necessary. The CytoSMART® Omni is a live-cell imaging system that scans entire culture vessels at regular intervals in the incubator. Because of its moving camera, the cells are undisturbed throughout the entire experiment.

In this study, a new high-throughput 3D wound healing model was developed. Different phases of the wound healing process were mimicked via different ratios of keratinocytes and fibroblasts. Wound healing was quantified via ring closure analysis of images obtained with the CytoSMART® Omni and ECM production after 24 hours.

Methods

Normal Human Dermal Fibroblasts (NHDF or F; C-12302; PromoCell) were cultured in Fibroblast Growth Medium 2 (C-23020; PromoCell). NHDFs were detached with trypsin and used at passage 6. Normal Human Epidermal Keratinocytes (NHEK or K; C-12003; PromoCell) were cultured in Keratinocyte Growth Medium 3 (C-20021; PromoCell) and detached with the detachkit (C-41200; PromoCell). NHEK were used at passage 5. For bioprinting 3D cell constructs, cells need to be magnetically labelled. Magnetic labelling was done by adding 600 µl Nanoshuttle (Nanoshuttle™-PL; 657843; Greiner Bio-One) per T75 flask and incubating overnight. ECM

production was activated by levitation. Levitation was performed by placing a levitation plate on a cell-repellent 6-well plate (657825; Greiner Bio-One) seeded with NHDF's or NHEK's ($1,6 \times 10^6$ cells/ml) for either 1 or 16 hours, respectively. The levitation time differs between cell types since splitting of the levitated dots can be harmful for sensitive cells. Thereafter, cells were resuspended and co-cultured in a cell-repellent 384-well plate (80 000 cells/well). The cells were seeded in the following co-culture ratios: (1) 1F:1K, (2) 3F:1K, (3) 1F:0K, (4) 1F:3K, (5) 0F:1K, in 75% Keratinocyte Growth Medium 3 and 25% Fibroblast Growth Medium 2. Next, the well plate was placed

on top of a 384-magnetic ring drive (655850; Greiner Bio-One) for 1 hour to create rings mimicking dermal wounds. Thereafter, the plate was placed on the CytoSMART® Omni to obtain high-resolution images at 37°C and 5% CO₂ (Fig. 2). Images were automatically uploaded to the CytoSMART® Cloud, where the internal ring areas were determined every hour, for 24 hours.

Statistical analysis was performed with GraphPad Prism. Differences in wound closure were measured via one-way ANOVA, followed by a Tukey's multiple comparisons test. Differences were considered significant for $P < 0.05$.



Fig. 2: (A) A 96-well plate placed on the CytoSMART® Omni inside a humidified incubator. (B) 3D ring construct representing a dermal wound.

Results

Wound closure was significantly slower for cell cultures with keratinocytes (3F:1K; 1F:1K; 1F:3K; 0F:1K) compared to the monoculture of fibroblasts (1F:0K). After 3 hours, the

percentage of wound closure was significantly lower for all groups which contained keratinocytes compared to the group with only fibroblasts. The longer the incubation time, the

smaller the differences between groups became. However, all groups with 50% or more keratinocytes had a significantly lower percentage of wound closure at all time points (Fig. 3).

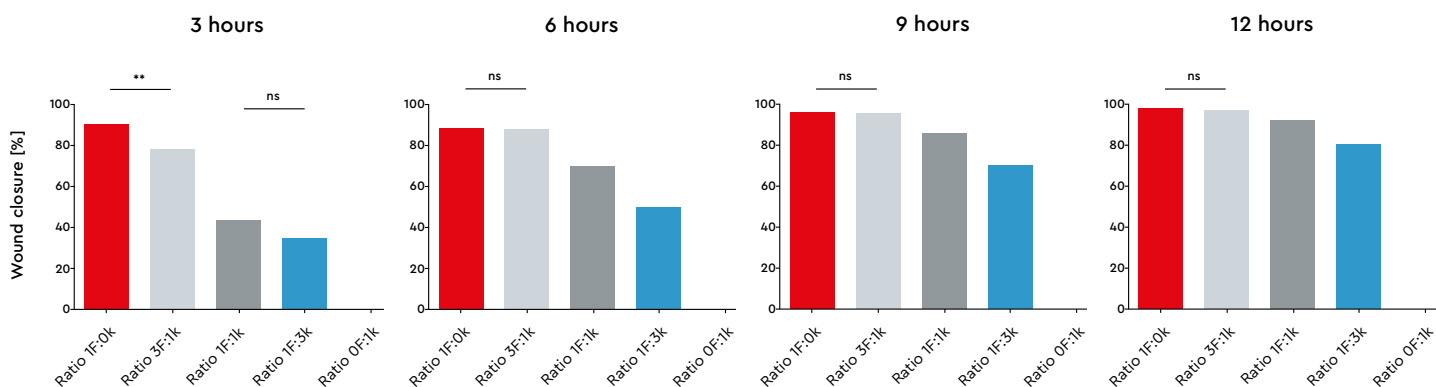


Fig. 3: Difference in percentage of wound closure at (A) 3, (B) 6, (C) 9 and (D) 12 hours. 'ns': no significant differences, ** $P \leq 0.01$. All other groups are significant different from each other ($P \leq 0.001$; 1F:0K: $n=45$, 3F:1K: $n=57$, 1K:1F: $n=50$, 1F:3K: $n=26$, 1K:0F: $n=36$).

The results of the GAG assay and collagen staining (n=2) after 24 hours were in line with the trends described in literature (Fig. 1 and Fig. 4). The production rate of both collagen

and GAG decreased when the percentage of keratinocytes in the co-culture increased (Fig. 4). For the 0F:1K samples, no GAG production was detected. This feature is also

seen in Figure 1, in the maturation phase, the GAG production stops for monocultures of keratinocytes.

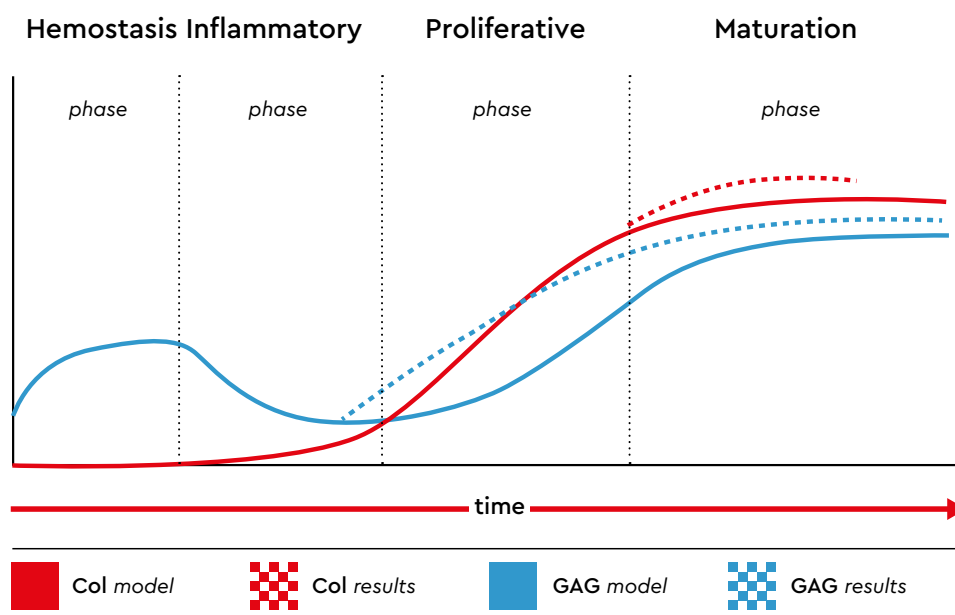


Fig. 4: The amount of GAG and collagen (Col) from the GAG assay and collagen staining (dotted lines) compared to the results from the model (Fig. 1). Collagen was not measured for all the ratios or wound healing phases. Statistical analysis was not performed (n=2).

Discussion

To develop new wound healing therapies, 3D *in vitro* wound healing models are needed to understand the continuous wound healing process. 3D models are often high in costs, highly laborious and low-throughput. The 'magnetic cell culture technique' developed by Greiner Bio-One enables relatively easy and low laborious development of 3D ring constructs. To analyze the continuous wound healing process, a high temporal resolution is required, which is achieved by live-cell imaging with the CytoSMART® Omni. In addition, the CytoSMART® Omni can be placed inside the incubator. This prevents contamination during imaging outside the humidified environment and creates a stable environment in which kinetic data can be obtained. The CytoSMART® Omni automatically image and analyze wound closure every hour in each well of a 384-well plate, resulting in a high-throughput 3D

wound healing model.

This study showed that the continuous wound healing process can be mimicked via co-cultures of fibroblasts and keratinocytes. The speed and percentage of wound closure increased upon increasing numbers of fibroblasts in the co-culture. These co-cultures have been shown to represent the proliferative phase of the wound healing process. In the maturation phase, however, the main goal of the wound healing process changes from ECM production and wound closure to maturation of the neo-ECM, in which the keratinocytes play a big role. This can also be seen in the co-cultures with a high number of keratinocytes, which are low in contractility and ECM production. These constructs, therefore, represent the maturation phase of the wound healing process.

By creating 3D ring constructs with the

different co-culture compositions in a 384-well plate, a high-throughput 3D wound healing model was made. Especially during the first 6 hours, the speed and percentage of wound closure were highly dependent on the co-culture ratio. In case only end-point measurements were taken, these results would not have been discovered. This study showed that using a monoculture or a one-ratio co-culture can only provide information on a small part of the wound healing process. In the wound healing process, the production of collagen and GAG is crucial to develop healthy tissue. The production rates of both are dependent on the specific wound healing phases. Preliminary results of our 3D wound healing model showed both GAG and collagen production in the model system corresponding to the production rates per wound healing phase described in the literature.

Conclusion

A low laborious and high-throughput 3D *in vitro* wound healing model was developed using the 'magnetic cell culture technique' from Greiner Bio-One and the CytoSMART®

Omni using PromoCell keratinocytes and fibroblasts in the respective medium. This 3D *in vitro* wound healing model can mimic the different phases of the wound healing process

based on the number of fibroblast and keratinocytes and the production rate of GAG and collagen. Therefore, this model can be highly efficient in drug screens for wound healing.

References

1. J R Dias, PL Granja, and PJ B'artolo. Advances in electrospun skin substitutes. *Progress in Materials Science*, 84:314–334, 2016.
2. Oryan, A., Alemzadeh, E., & Moshiri, A. (2017). Burn wound healing: present concepts, treatment strategies and future directions. *Journal of wound care*, 26(1), 5–19.
3. Zielins, E. R., Brett, E. A., Luan, A., Hu, M. S., Walmsley, G. G., Paik, K., ... & Longaker, M. T. (2015). Emerging drugs for the treatment of wound healing. *Expert opinion on emerging drugs*, 20(2), 235–246.
4. Anna T Grazul-Bilska, Mary Lynn Johnson, Jerzy J Bilski, Dale A Redmer, Lawrence P Reynolds, Ahmed Abdullah, and Kay M Abdullah. Wound healing: the role of growth factors. *Drugs Today (Barc)*, 39(10):787–800, 2003.
5. Marta Kapa lczyńska, Tomasz Kolenda, Weronika Przyby la, Maria Zajaczkowska, Anna Teresiak, Violetta Filas, Matthew Ibbs, Renata Bliźniak, Lukasz Luczewski, and Katarzyna Lamperska. 2d and 3d cell cultures—a comparison of different types of cancer cell cultures
6. Kritika Iyer, Zhuo Chen, Teja Ganapa, Benjamin M Wu, Bill Tawil, and Chase S Linsley. Keratinocyte migration in a three-dimensional *in vitro* wound healing model co-cultured with fibroblasts. *Tissue engineering and regenerative medicine*, 15(6):721–733, 2018

About the Author

Linda Boekestijn is an Application Scientist at CytoSMART Technologies, a company specialized in the development and manufacturing of smart microscope systems for life science laboratories. The company was founded in

2012 by a team of biologists and engineers who were convinced that a new generation of miniaturized microscopes, powered by artificial intelligence for image analysis, would allow biologists to make discoveries more efficiently

and at scale. In 2018 CytoSMART was selected by Microsoft for its prestigious Scale Up program. CytoSMART's microscopy solutions are used in research laboratories worldwide. www.cytosmart.com



PromoCell GmbH
Sickingenstr. 63/65
69126 Heidelberg, Germany
info@promocell.com
www.promocell.com



CytoSMART Technologies B.V.
Emmasingel 33
5611 AZ Eindhoven, The Netherlands
info@cytosmart.com
www.cytosmart.com